Electronic Supplementary Material (ESI) for ChemComm.
This journal is © The Royal Society of Chemistry 2021

Precisely Tuning the Electronic Structure of Structurally PtCoFe Alloy via Dual-components Promoter for Oxygen Reduction

Qingmei Wang[a], Hao Tang [a], Meng Wang [a*], Lin Guo[b], Siguo Chen[a*],Zidong Wei[a]

[a] The State Key Laboratory of Power Transmission Equipment & System Security and New Technology, Chongqing Key Laboratory of Chemical Process for Clean Energy and Resource Utilization, School of Chemistry and Chemical Engineering, Chongqing University, Chongqing 400044, China.

[b] Key Laboratory of Photochemical Conversion and Optoelectronic Materials, Technical Institute of Physics and Chemistry, Chinese Academy of Sciences, Beijing 100190, China.

Corresponding Author: *csg810519@126.com; * wmeng@cqu.edu.cn

Experiment section

Chemicals and materials

Commercial Pt/C catalyst (JM, 20 wt. %), 4-(2-ethylamino) Benzene-1,2-diol ($C_8H_{11}O_2N$, 90%). Cobaltous Chloride ($CoCl_3$, 99%), Ferric chloride ($FeCl_3$,99%), Tetraethyl Orthosilicate ($Si(OC_2H_5)_4$ 98%), Tris(hydroxymethyl) Aminomethane ($C_4H_{11}NO_3$, 99.5%).

Preparation of ordered PtCoFe-1-X catalyst

100 mg commercial Pt/C catalyst (JM, 20 wt. % Pt) was dispersed in the solution mixtures of deionized water (20 mL) and ethanol (20 mL). The mixture was then stirred ultrasonically at room temperature for 1h to achieve homogeneous dispersion, and then 40 mg dopamine ($C_8H_{11}O_2N$, 90%) dissolved in 10ml Tris-HCl (50 mM, pH≈8.5, $C_4H_{11}NO_3$, 99.5%) solution was added. The mixture was stirred for 10 hours at room temperature. The obtained core-shell structured nanocomposite (Pt/C@PDA) was collected by centrifugation and washed with

deionized water and then dried at 80℃ for 6 h. The obtained Pt/C@PDA was stirred with 1.8ml 0.685M $CoCl_3$ solution and Xml 0.536M $FeCl_3$ solution in deionized water to form Pt/C@PDA-Co^{3+} suspension. After 20h stirring, solution of 5mL Tetraethoxysilane ($Si(OC_2H_5)_4$, TEOS, 98%) and 1ml HCl (pH=1) solution were added to the Pt/C@PDA-Co^{3+} Fe^{3+} suspension and the mixture was mixed at room temperature for 1h to get a homogeneous mixture. The homogeneous mixture was moved to glass petri dishes and allowed to slowly evaporate in empty environments until the composite films (Pt/C@PDA-$Co^{3+}Fe^{3+}$@SiO_2) formed. For pyrolysis of the Pt/C@PDA-$Co^{3+}Fe^{3+}$@SiO_2, the solid films were heated at a rate of 5℃/min to 700℃ and maintained for 4h under flowing 15%H_2/85%Ar to obtain pyrolyzed PtCoFe@SiO_2 composites. After cooling down the sample to room temperature, the PtCoFe@SiO_2 composites were etched by low concentration HF (0.1M) to removal the silica layers. The resulting PtCoFe-1-0.2 products were washed with anhydrous alcohol and deionized water and finally dried under vacuum at 80℃ for 12 h. For comparison, the related PtCoFe-1-0.2, PtCoFe-1-0.6 and PtCoFe-1-1 was prepared by adding 0.1ml, 0.3ml and 1ml 0.536M $FeCl_3$ solution, respectively. The Pt/Co/Fe molar composition in the as-prepared PtCoFe-1-0.2, PtCoFe-1-0.6 and PtCoFe-1-1 samples are measured to be 49/44/7, 49/39/12, 49/26/25, respectively, as determined by ICP-AES.

Preparation of ordered PtCo-X catalyst:

The overall prepared steps were the same as the mentioned before, except for the adding of extra $FeCl_3$ solution. For comparison, the related PtCo-1, PtCo-3, PtCo-5 and PtCo-7 were prepared by adding 1.8ml, 5.4ml, 9ml and 12.6ml 0.685M $CoCl_3$ solution, respectively. The Pt/Co molar composition in the as-prepared PtCo-1, PtCo-3 PtCo-5 and PtCo-7 samples are measured to be 56/44, 49/51, 45/55 and 42/58 respectively, as determined by inductively coupled plasma atomic emission spectrometer (ICP-AES).

Characterization

Transmission electron microscopy (TEM) was carried out on a Zeiss LIBRA 200 field-emission transmission electron microscope operating at 200 kV. High-angle annular dark-field scanning TEM (HAADF-STEM)-energy-dispersive X-ray spectroscopy (EDS) was carried out on a JEM-ARM200F transmission electron microscope operated at 300 kV. X-ray photoelectron spectroscopy (XPS) analysis was conducted on an ESCALAB250Xi spectrometer equipped with a monochromatic Al X-ray source (Al Kα, 1.4866 keV). X-ray diffraction data were collected on a PANalytical X' Pert powder diffractometer using Cu Kα radiation at a step rate of 2° min^{-1}. The elemental content of catalysts was determined by inductively coupled plasma mass spectrometry (Thermo Fisher Scientific, iCAP6300 ICP-MS).

Electrochemical measurements

The electrochemical experiments were conducted in a standard three-compartment electrochemical cell with a Pine rotating disk electrode (RDE) and a VersaSTAT 3F electrochemical workstation. An Ag/AgCl (3 M KCl) electrode and a platinum wire were used as reference and counter electrodes, respectively. All potentials in this study, however, are given relative to the reversible hydrogen electrode (RHE). The working electrodes were prepared by applying catalyst ink onto 5 mm glassy carbon (GC) disk electrodes. To prepare the working electrode, the catalyst was dispersed in ethanol and ultrasonicated for 30 min to form a uniform catalyst ink (from 0.5 to 1 mg Pt mL^{-1}). Afterwards, 5 to 10 μL of well-dispersed catalyst ink was applied onto a prepolished GC disk. After the ink had dried at room temperature, a drop of 0.05 wt% Nafion solution was applied onto the surface of the catalyst layer to form a thin protective film. The prepared electrodes were dried at room temperature before electrochemical tests.

Before electrochemical measurements, all electrodes were pretreated by being cycled between 0.04 and 1.2 V at a sweep rate of 50 mV s^{-1} for 70 cycles to remove any surface contamination. Electrochemically active surface area (ECSA) measurements were conducted by CO stripping (electro-oxidation of adsorbed CO) at room temperature in N_2-saturated 0.1 M $HClO_4$ solution. Oxygen reduction reaction (ORR) measurements were conducted in O_2-saturated 0.1 M $HClO_4$ solution that was purged with oxygen during the measurements. The rotation speed was controlled at 1600 rpm. The scan rate for ORR measurements was 10 mV/s. The ORR polarization curves were collected at 1600 rpm. The current densities for ORR were corrected by ohmic iR drop compensation during the measurements. The accelerated durability test (ADT) was performed at room temperature in oxygen-saturated 0.1 M $HClO_4$ solution by applying cyclic potential sweeps between 0.6 and 1.1 V at a sweep rate of 50 mV s^{-1} for 30,000

CV cycles. For comparison, a commercial Pt/C catalyst (JM, 20 wt.% Pt, Pt particle size: 2-4 nm) was used as the baseline catalyst, and the same procedures as previously described were used to conduct the electrochemical measurement. The Pt loading on the RDE working electrode was determined by ICP-MS.

The ECSA of Pt in the catalysts was calculated using the following equations:

$$ECSA - CO = \frac{Q_{CO}}{0.42 \times [Pt]} \tag{1}$$

Where Q_{CO} (mC) is the electro-oxidation of adsorbed CO, 0.42 mC cm^{-2} is the electrical charge associated with monolayer adsorption of CO on Pt, and [Pt] is the loading of Pt on the working electrode.

The specific kinetic current densities (j_k) associated with the intrinsic activity of the catalysts can be obtained by Eq. (2):

$$j_k = \frac{j_d \times j}{j_d - j} \tag{2}$$

Where j is the measured current density, j_k is the kinetic current density, and j_d is the diffusion-limited current density.

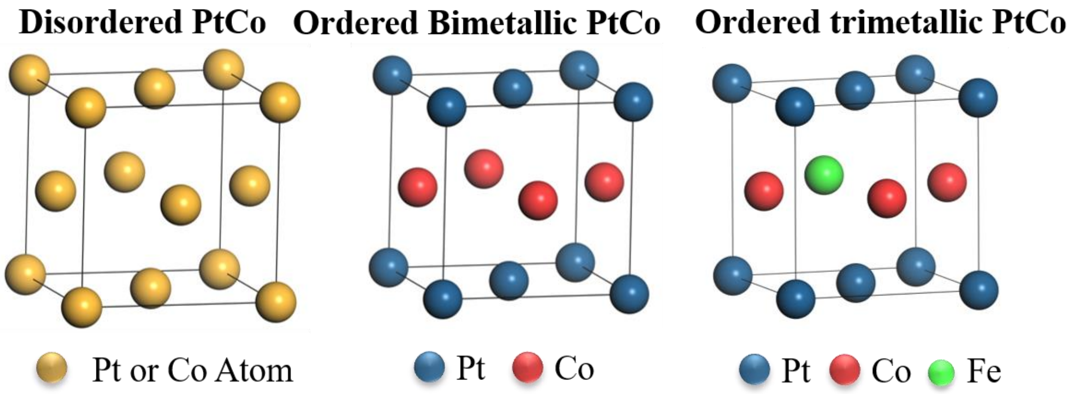

Figure S1. The unit-cell structure simulation of (b) intermetallic L1$_0$-PtCo and (c) trimetallic L1$_0$-PtCoFe.

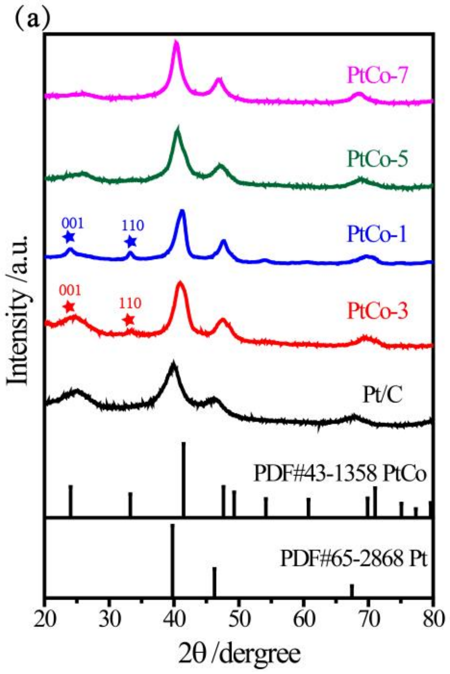

Figure S2. XRD patterns for PtCo-X (X = 1, 3, 5 and 7) and commercial Pt/C respectively and the standard PDFs of PtCo (PDF#43-1358) and Pt (PDF#65-2868).

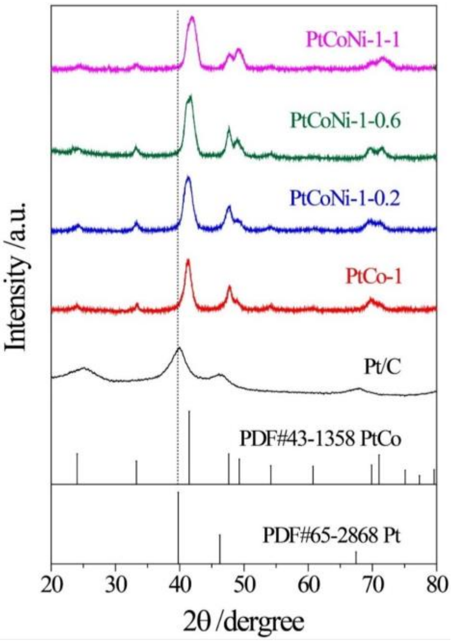

Figure S3. The XRD patterns for PtCoNi-X (X = 0.2, 0.6 and 1), $L1_0$-PtCo-1 and commercial Pt/C catalysts respectively and the standard PDFs of PtCo (PDF#43-1358) and Pt (PDF#65-2868).

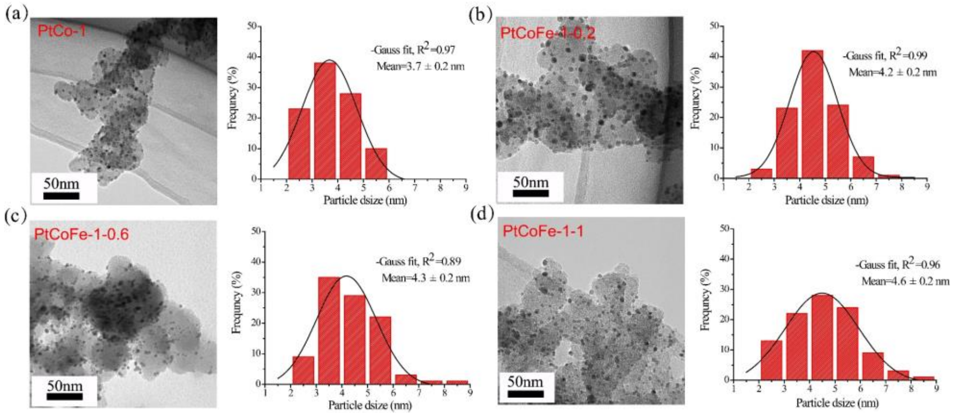

Figure S4. The overall TEM images and corresponding particle distribution histograms of the bimetallic L1_0-PtCo-1 (a), L1_0-PtCoFe-1-0.2 (b), L1_0-PtCoFe-1-0.6 (c) and L1_0-PtCoFe-1-1 catalyst (d) after high temperature annealing.

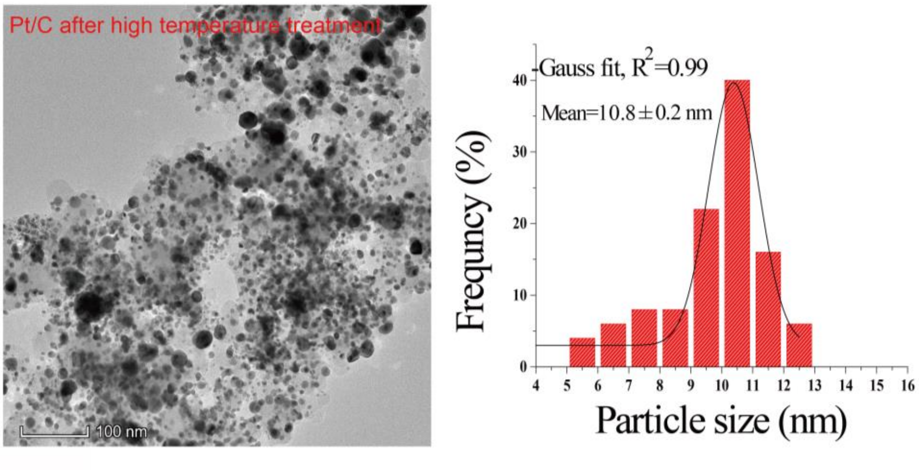

Figure S5. The overall TEM images and corresponding particle size statistics of the commercial Pt/C catalysts after high temperature annealing.

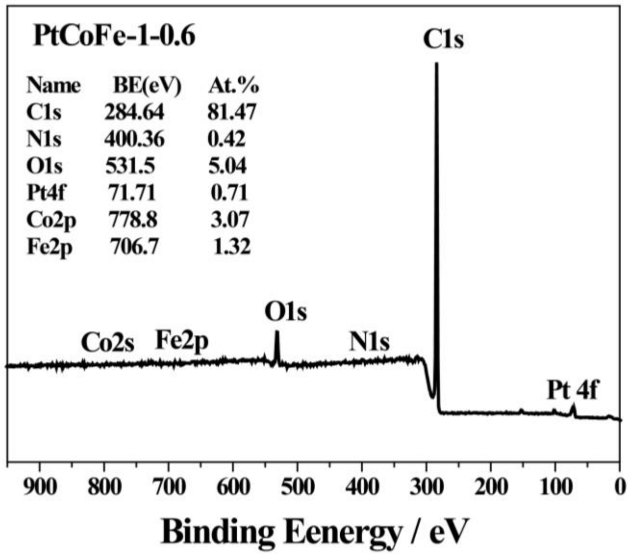

Figure S6. The XPS survey of the as-prepared L1$_0$-PtCoFe-1-0.6 catalysts.

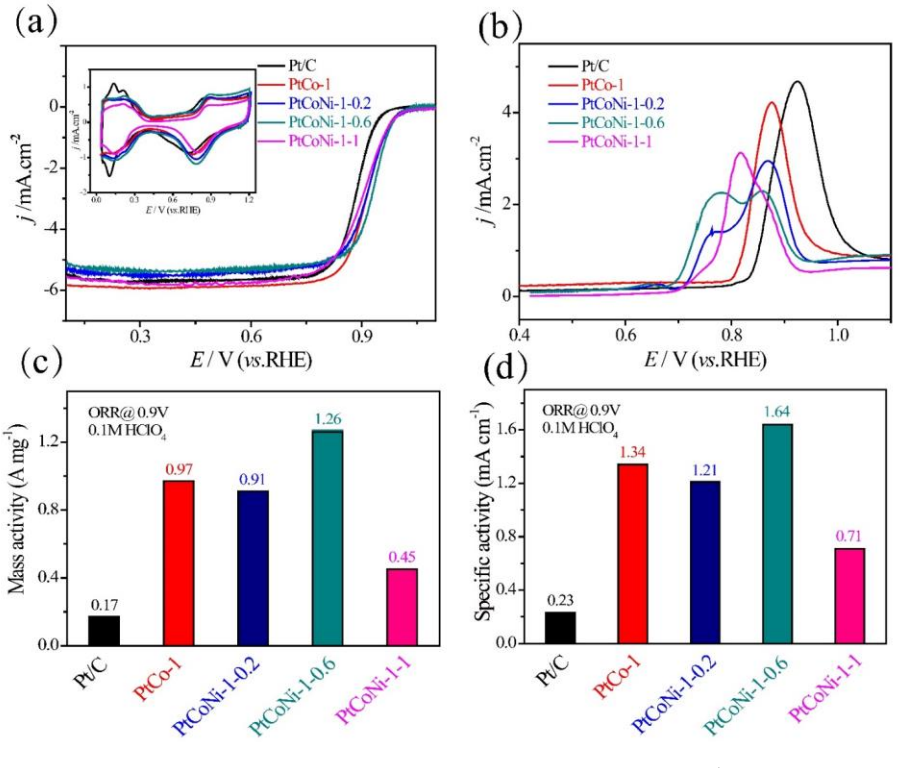

Figure S7. (a) ORR polarization curves and (b) CO stripping curves of trimetallic L1$_0$-PtCoNi-1-X (X=0.2, 0.6 and 1), L1$_0$-PtCo-1 and Pt/C catalysts recorded in O_2-saturated 0.1 M $HClO_4$ solution at sweep rate of 10 mV/s and a rotation rate of 1600 rpm, the insert show the CV curves recorded in N_2 purged 0.1 M $HClO_4$ solution at a scan rate of 50 mV/s and corresponding (c) mass activity and (d) Specific activity at 0.9 V vs RHE

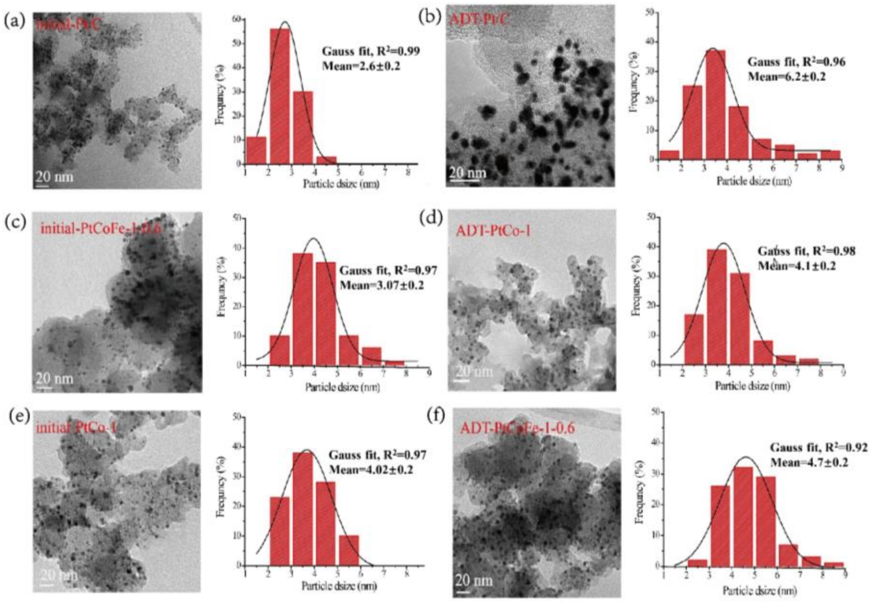

Figure S8. The TEM images and particle-distribution histograms of initial Pt/C before (a) and after (b) 20,000 CV cycles, L1$_0$-PtCo-1 before (c) and after (d) 20,000 CV cycles, L1$_0$-PtCoFe-1-0.6 before (e) and after (f) 20,000 CV cycles between 0.6 and 1.1 V in O_2-saturated 0.1 M $HClO_4$ at a scan rate of 50 mV s^{-1}.

Sample	I_{110}/I_{111}	I_{001}/I_{111}	Lattice Strain%
PtCo(PDF#43-1358)	**0.25**	**0.36**	**----**
PtCo-1	**0.17**	**0.18**	**1.51**
PtCoFe-1-0.2	**0.15**	**0.22**	**1.66**
PtCoFe-1-0.6	**0.19**	**0.28**	**1.74**
PtCoFe-1-1	**0.16**	**0.23**	**1.62**

Table S1. The detailed ordered degree and alloy degree for L1$_0$-PtCoFe-X (X = 0.2, 0.6 and 1) and L1$_0$-PtCo-1 as compared to the standard PDFs of PtCo (PDF#43-1358) from the XRD patterns, respectively.

Catalysts	ICP Loading by weight%			Atomic molar ratio (approximation)	EDX Loading by weight%			Atomic molar ratio (approximation)
	Pt	Co	Fe	Pt/Co/Fe	Pt	Co	Fe	Pt/Co/Fe
PtCoFe-1-0.2	**49.2**	**44.1**	**6.7**	**0.25/0.75/0.11**	**54.2**	**34.5**	**11.3**	**0.28/0.59/0.20**
PtCoFe-1-0.6	**49.5**	**39.1**	**11.4**	**0.25/0.66/0.20**	**55.2**	**24.5**	**20.3**	**0.28/0.42/0.36**
PtCoFe-1-1	**49.3**	**25.8**	**24.9**	**0.25/0.44/0.44**	**51.4**	**20.8**	**27.8**	**0.26/0.35/0.50**
PtCo-1	**53.2**	**46.8**	**---**	**0.27/0.79**	**55.8**	**44.2**	**---**	**0.29/0.75**

Table S2. The elemental loadings of PtCoFe-1-0.2, PtCoFe-1-0.6 and PtCoFe-1-1 catalysts by weight percent of Pt, Co and Fe using ICP (with respect to each element) and by EDX.

Item	unit	Pt/C	PtCo -1	PtCoFe -1-0.2	PtCoFe -1-0.6	PtCoFe -1-1
Mass activity @0.9V_{IRfree}	A/m_{Pt}	0.17	0.97	0.9	1.43	0.74
Specific activity @0.9V_{IRfree}	mA/cm^2	0.23	1.34	1.41	2.23	1.35
ECSA-CO	m^2/g	69	71	75	79	73

Table S3. The ECSA-CO, half-wave potential, and the calculated mass activity and specific activity at 0.9V of the $L1_0$-PtCoFe-X (X = 0.2, 0.6 and 1), $L1_0$-PtCoNi-X (X = 0.2, 0.6 and 1) and $L1_0$-PtCo-1 as compared to the commercial Pt/C, respectively.

	Mass activity (A/mgPt) @0.9V	Specific activity (mA/cm^{-2}) @0.9V	Ref
PtCo/G-600	**0.952**	**0.524**	**1**
PtPdNi	**1.14**	**1.52**	**2**
$Pt_4PdCu_{0.4}$	**1.09**	**2.21**	**3**
PtCoAu/C	**0.69**	**1.73**	**4**
PtPbAu	**0.59**	**0.42**	**5**
PtPdIr	**0.52**	**0.82**	**6**
PtCoFe/NPG	**1.15**	**---**	**7**
PtAuNi/C	**0.83**	**1.1**	**8**
PtCo-1	**0.97**	**1.34**	**This Work**
PtCoFe-1-0.2	**0.90**	**1.41**	**This Work**
PtCoFe-1-0.6	**1.43**	**2.23**	**This Work**
PtCoFe-1-1	**0.74**	**1.35**	**This Work**

Table S4. A brief comparison of the ORR electrochemical activity of the catalysts reported in the currently literature to the as-prepared PtCoFe catalyst.

Catalysts	**ICP Loading by weight% Before ADT**			**ICP Loading by weight% After ADT**		
	Pt	**Co**	**Fe**	**Pt**	**Co**	**Fe**
PtCoFe-1-0.2	**49.2**	**44.1**	**6.7**	**50.9**	**42.8**	**6.3**
PtCoFe-1-0.6	**49.5**	**39.1**	**11.4**	**49.8**	**39.0**	**11.2**
PtCoFe-1-1	**49.3**	**25.8**	**24.9**	**50.3**	**25.5**	**24.2**
PtCo-1	**53.2**	**46.8**	**---**	**53.8**	**46.2**	**---**

Table S5. The elemental loadings of PtCoFe-1-0.2, PtCoFe-1-0.6 and PtCoFe-1-1 catalysts of Pt, Co and Fe before and after ADT using ICP and by EDX.

Reference:

1. Chunyong He, Shengkai Zhang, Juzhou Tao, Pei Kang Shen, One-step solid state synthesis of PtCo nanocubes/graphene nanocomposites as advanced oxygen reduction reaction electrocatalysts, Journal of Catalysis 362 (2018) 85-93.
2. Hongjing Wang, Yinghao Li, Kai Deng, Chunjie Li, Hairong Xue, Ziqiang Wang, Xiaonian Li, You Xu, and Liang Wang, Trimetallic PtPdNi-Truncated Octahedral Nanocages with a Well-Defined Mesoporous Surface for Enhanced Oxygen Reduction Electrocatalysis, ACS Appl. Mater. Interfaces 2019, 11, 4252-4257.
3. Wei Ye, Shuangming Chen, Mengshan Ye, Chenhao Ren, Jun Ma, Ran Long, Chengming Wang, Jian Yang, Li Song, Yujie Xiong, $Pt_4PdCu_{0.4}$ alloy nanoframes as highly efficient and robust bifunctional electrocatalysts for oxygen reduction reaction and formic acid oxidation, Nano Energy 39 (2017) 532-538.
4. Li-Ming Guo, Dong-Feng Zhang, Lin Guo, Structure Design Reveals the Role of Au for ORR catalytic Performance Optimization in PtCo-Based Catalysts, Adv. Funct. Mater. 2020, 30, 2001575.

5. Xiang Zhang, Shibin Wang, Chenshuo Wu, Hong Li, Yi Cao, Shenggang Liand Haibing Xia, Synthesis of S-doped AuPbPt alloy nanowirenetworks as superior catalysts towards the ORR and HER, J. Mater. Chem. A, 2020, 8, 23906.
6. Jiawei Zhu; Minghao Xie; Zitao Chen; Zhiheng Lyu; Miaofang Chi; Wanqin Jin; Younan Xia, Pt-Ir-Pd Trimetallic Nanocages as a Dual Catalyst for Efficient Oxygen Reduction and Evolution Reactions in Acidic Media, Adv. Energy Mater. 2020, 10, 1904114.
7. Xing Zhong, Wenlei Xu, Lei Wang, Yingying Qin, Guilin Zhuang, Xiaonian Li, Jian-guo Wang, Twin-like ternary PtCoFe alloy in nitrogen-doped graphene nanopores as a highly effective electrocatalyst for oxygen reduction, Catal. Sci. Technol., 2016,6, 5942-5948.
8. Fei Liu, Kui Sun, Zhiyan Rui, Jianguo Liu, Tian Juan, Ruirui Liu, Jun Luo, Zhongwei Wang, Yingfang Yao, Lin Huang, Peng Wang, Zhigang Zou, Highly Durable and Active Ternary Pt-Au-Ni Electrocatalyst for Oxygen Reduction Reaction, ChemCatChem, 2018,10,3049-3056.